

OBSERVATIONS OF LPH 123 AND 127, HIGH-MASS X-RAY
BINARIES, IN A TWO-SUMMER ATTEMPT TO DETECT
VARIABILITIES

by

McKay E. Bonham

A senior thesis submitted to the faculty of

Brigham Young University

in partial fulfillment of the requirements for the degree of

Bachelor of Science

Department of Physics and Astronomy

Brigham Young University

August 2008

Copyright © 2008 McKay E. Bonham

All Rights Reserved

BRIGHAM YOUNG UNIVERSITY

DEPARTMENT APPROVAL

of a senior thesis submitted by

McKay E. Bonham

This thesis has been reviewed by the research advisor, research coordinator, and department chair and has been found to be satisfactory.

Date

Eric Hintz, Advisor

Date

Eric Hintz, Research Coordinator

Date

Ross Spencer, Department Chair

ABSTRACT

OBSERVATIONS OF LPH 123 AND 127, HIGH-MASS X-RAY BINARIES, IN A TWO-SUMMER ATTEMPT TO DETECT VARIABILITIES

McKay E. Bonham

Department of Physics and Astronomy

Senior Thesis

Star J2030.5+4751, also known as star 123 of the LPH catalogue, and star 2202+501, also known in the LPH catalogue as 127, are high-mass X-ray binaries. Late B-type stars that are part of high-mass X-ray binary systems are likely to be variable stars with a long period. We are studying these systems with the intent of identifying them as variable stars and discovering their period. Our studies have been in the form of differential photometry, which attempts to spot variations in these stars' magnitude by comparing them with stable stars in their frames. We have seen interesting variations in these stars, but not repeating variations that could be used to determine a period. We conclude that more data, gathered on a much more regular schedule, will be required to reach conclusive results about the variability of these targets. We also report a dramatic shift in the magnitude of one of LPH 123's neighbors, and present it as a candidate for further variable star research.

ACKNOWLEDGMENTS

Special thanks go to Dr. Hintz for his help in many stages of this project. He recommended this topic to me for my research efforts, gave me guidance in reducing and analyzing my data, helped edit this paper, and also acted as a consultant whenever I had any questions about any aspect of the involved astronomy. Noel Barragan, Larry Camarota, Tiffany Brown, Jessica Bugno, Chris Draper, Janalee Harrison, Amanda Henderson, Christie Pennington, Natalie Porter, Jeremy Schoonmaker, Kent Slack, and Craig Swenson all operated the telescope on nights when my data was collected, and I very much appreciate their assistance in enlarging the quantity of my information. I am glad I was also able to collect data to contribute to some of their observing projects. I would also like to thank Professor Mike Joner, Craig Swenson, and E. Paul Iverson for their work on the SIDAP script package, and especially for their efforts to help me troubleshoot as I worked with these scripts.

Contents

Acknowledgments	v
Table of Contents	vi
List of Tables	viii
List of Figures	ix
1 Introduction and Background	1
1.1 Background on HMXBs	1
1.2 Background on Variable Stars	2
1.3 Previous Research	3
1.4 Basic Background Information on Targets	4
1.5 Motivation	5
2 Data Reduction, and Photometry	7
2.1 Reduction	7
2.2 Photometry	8
2.2.1 Aperture Photometry	8
2.2.2 Differential Photometry	9
2.3 Telescope and Camera Information	9
3 Data Analysis	10
3.1 Data Acquisition	10
3.2 Reduction by Script	12
3.3 Statistical Analysis	15
3.4 Initial Analysis	15
3.5 Unusually Noisy Data	18
3.6 Multiple-Night Analysis	22

3.7	Phased Analysis	24
3.8	Additional Graphs	27
4	Conclusions	32
4.1	Results	32
4.2	Further Research	32
	References	32
A	Period04 Log Excerpts	34

List of Tables

3.1	Summary of Data Collected	11
3.1	Summary of Data Collected	12
3.2	Summary of Data Reduced and Analyzed	12
3.3	Comparison Stars Retained by VARSTAR	16

List of Figures

1.1	Star field of LPH 123	4
1.2	Star field of LPH 127	5
3.1	Typical Night of Varstar Results	17
3.2	Typical Light Curve for One Night of LPH 123	18
3.3	More Nights that Aren't β Cephei Variables	19
3.4	Typical Night of Varstar Results, Other Star	20
3.5	A Strange Quantity of Clear Outliers	21
3.6	Multiple Nights Makes Outliers Stand Out Too Much	22
3.7	Zeropoint Adjustments for LPH 123	23
3.8	Zeropoint Adjustments for LPH 127	24
3.9	Overall Graph of LPH 123	25
3.10	Overall Graph of LPH 127	26
3.11	Median Points of LPH 123	27
3.12	Median Points of LPH 127	28
3.13	Phased Light Curve of LPH 123	28
3.14	Phased Light Curve of LPH 127	29
3.15	Phased Light Curve of a Suspect Comparison Star	29
3.16	LPH 123 - Separated by Year	30
3.17	Comparison Star 5: Located in Frame and Light Curve 2007	30
3.18	LPH 127 - Second Summer Only	31
A.1	Period04 Log for LPH 123	34
A.2	Period04 Log for LPH 127	35

Chapter 1

Introduction and Background

1.1 Background on HMXBs

High-mass X-ray binaries (HMXB) are systems in which a large O or B star is orbited by a compact object companion, namely a neutron star or black hole. Matter accretes from the star to the compact object, and the conversion of the accreting matter's gravitational energy to electromagnetic energy results in X-ray radiation, which makes HMXBs some of the brightest X-ray sources in the celestial sphere.

In 2000, a number of bright X-ray sources were studied by Liu, van Paradijs, and van den Heuvel. Those which were determined to be high-mass X-ray binaries were published as the LPH catalogue (Liu et al. (2007)).

Finding Periods in High Mass X-Ray Binaries, a 2006 paper by Gordon Sarty, László L. Kiss, Helen M. Johnston, Richard Huziak, and Kinwah Wu, issued a call to amateur astronomers to identify the periods of variability of a number of objects in the LPH catalogue (Sarty et al. (2007)). This paper detailed the formation process of HMXBs, properties they are expected to have as a result of this formation process, and a number of reasons they are likely to be variable objects. They divide their explanation between SG/X-ray binaries, in which the two objects started out relatively close together, and Be/X-ray binaries, in which they were relatively far apart. As our targets of study were both of the latter variety (spectral types B0.5V-IIIe and Be), we shall focus on the properties that are expected in these longer-period HMXBs.

The system's compact object was formed in a type Ib supernova. Its companion star survived this supernova, but the shockwave produced perturbed the star into a highly eccentric orbit. The star is expected to be extremely oblate, to the point of having an "equatorial disk"; this is due to B stars' tendency to rotate quickly in general, as well as the additional tidal effect caused by the compact object companion.

This equatorial disk, in addition to the solar wind normally generated by a massive star (between 8 and $15M_{\odot}$), provides the means for matter to escape the star and form an accretion disk around the compact object in spite of the relatively wide orbit between the two objects, especially when the two of them are near periastron, their point of closest approach.

1.2 Background on Variable Stars

Objects whose luminosity varies in our sky are diverse. Variable stars can have extrinsic variability, intrinsic variability, or both. Extrinsic variability means the star varies only because of the way in which we view it from our Earthly vantage point. For example, eclipsing binary stars are extrinsic variables. Intrinsic variables actually vary in luminosity over time, due to some kind of physical change in the stars themselves. For example, δ Scuti variables and other pulsators are intrinsic variables. Variable stars are also classified in a number of other ways, depending on their period or amplitude of variability, their spectral type or size, their chemical composition, or other circumstances. The right spectral type or other trait can make a star a good “candidate” for being a variable star, even if no variability has yet been observed. There are a number of reasons why HMXBs are good candidates for being variables.

In a long-period HMXB, the oblate B star is likely to manifest “ellipsoidal variation,” or a change in apparent surface area from our perspective depending on whether we are facing its equator or its pole at different parts of its orbit. This effect should be especially strong if the star fills or nearly fills its Roche lobe. This would make the star an extrinsic variable.

If the accretion disk of an HMXB’s compact object radiates enough X-ray radiation, it could heat the near side of its companion enough to make that side of the star brighter than the far side. The star would appear to us to grow brighter and dimmer depending on which side of it was facing us. This is another example of how an HMXB could be an extrinsic variable. This type of variability is more likely in

an SB/X-ray binary, but it could happen in a Be/X-ray binary, in spite of the wide orbit, if the black hole or neutron star is massive enough.

An HMXB could also be an intrinsic variable. The X-ray emissions of an HMXB are known to increase when the system is near periastron. It seems likely that periastron could also cause greater emissions in the visible spectrum, especially if the system’s ambient matter can absorb some of the X-rays and emit visible light in return.

The star of an HMXB could simply be a β Cephei pulsator. Its size and spectral type are agreeable to this type of variability.

An HMXB could simply be an eclipsing system from our point of view. This would change its apparent luminosity at least a little bit, as its compact object would block some of the light from the star. This effect would probably be more dramatic in the X-ray spectrum than in the visible light spectrum, as the star would block line of sight to the accretion disk, where the X-rays originate, during an eclipse.

[Sarty et al. \(2007\)](#) mention a few less likely possible causes for variability in an HMXB, but they name the first three reasons identified above as the most likely possibilities. They neglect to mention the possibility of a β Cephei at all.

1.3 Previous Research

In Finding Periods in High Mass X-Ray Binaries, [Sarty et al. \(2007\)](#) list 47 stars from the LPH catalogue, including 123 and 127, that are their “program stars” ([Sarty et al. \(2007\)](#)). These are targets that they state have known optical counterparts, as opposed to X-ray sources that act like HMXBs but for which we can’t actually identify one visible star as the origin. They state that all of their program stars have unknown orbital periods. They state that they already have some photometric data for LPH 123 and 127, but we did not have access to their data and did not use it in our analysis.

1.4 Basic Background Information on Targets

LPH 123 is also known as AAVSO 2157+49, J2030.5+4751, or SAO 49725. It is located in the constellation Cygnus near Deneb, with a right ascension (RA) of 20 hrs 30 min 30 sec and a declination (δ) of $+47^\circ 51' 51''$. Its spectral type is B0.5V-IIIe, and it has a listed visual magnitude of 9.27 mag. Figure 1.1 shows the star field of LPH 123, with LPH 123 itself centered.

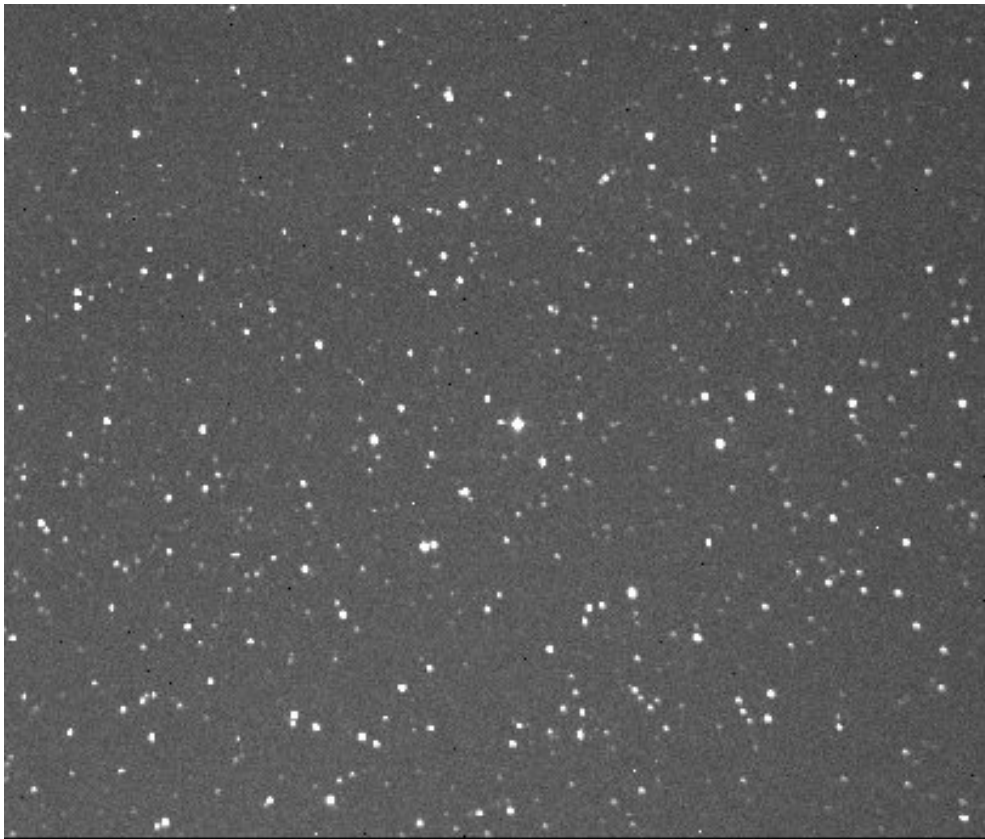


Figure 1.1: LPH 123 is the star in the center of the frame.

LPH 127 is also known as 2202+501, AAVSO 2157+49, SAO 51568, or V2157 Cyg. It is located in the constellation Cygnus near the borders of Cepheus and Lacerta, with a right ascension (RA) of 22 hrs 01 min 38 sec and a declination (δ)

of $+50^{\circ} 10' 05''$. Its spectral type is Be, and it has a listed visual magnitude of 8.80 mag. Figure 1.2 shows the star field of LPH 127, with LPH 127 itself centered.



Figure 1.2: LPH 127 is the star in the center of the frame.

1.5 Motivation

Learning about the periodicity of HMXBs could confirm our models of how such systems formed and the properties they have. This, in turn, could help us learn more about Type 1b Supernovas or even about compact objects and the way they

form accretion disks. Establishing the period of more HMXBs could also give them more status as a separate category in variable star research.

Chapter 2

Data Reduction, and Photometry

2.1 Reduction

The great challenge of differential photometry is minimizing any effects that could alter the apparent amount of light coming from your intended target, and coming from its neighbors that you are using to compare it to. What makes this difficult, besides the atmosphere, is the impossibility of having a perfect camera. Therefore, we use data reduction to mitigate the effects of camera imperfections.

The photon detectors used in modern astronomical research dealing with visible light are called charge-coupled devices (CCDs). CCDs are also at the heart of modern digital cameras and video cameras. Astronomical CCDs are of exceptional quality, able to collect over 75% of photons that strike their pixels at most wavelengths. Unfortunately CCDs aren't perfect. There are three ways in particular they can lead to distortions in the number of photons counted on each pixel of an astronomical frame.

First, each pixel of a CCD has a distinct zero point. If you think of the CCD as an array of buckets that catch drips of water, this is like the buckets having their bottoms at different depths, and our pictures are based on the final height that the water attains within each bucket. To correct for this problem, we take pictures with an exposure time of zero seconds. These pictures are called bias frames or zero frames.

Second, the CCD can give us false results if it picks up photons from somewhere other than the area our telescope is pointed at. The telescope should minimize any ambient light from its surroundings, except from the area of the sky we aim at, but this does not stop photons that are generated within the telescope itself, due to its internal electronics. To correct for errors caused by these electronically generated

photons, we have the telescope take pictures with its shutter closed, so it only picks up the photons that are internally generated. These pictures are called dark frames.

Third, when the CCD's pixels are struck by photons, they have individual response rates to this input. Some are more sensitive than others. To correct for this source of error, we take pictures of uniform fields. These pictures are called flat frames. This is done by aiming the telescope at a blank area of the sky when it is dark enough to not damage the CCD with overload, but light enough that no stars are visible.

Armed with zero frames, dark frames, and flat frames, collectively called calibration frames, we can adjust our pictures of astronomical objects, or object frames, to compensate for these three major sources of error. Zeros and darks are subtracted from the flat frames, while flat frames are scaled to an average value of one and are divided out of the object frames. This leaves us with frames that, hopefully, represent actual ratios of photons collected by different pixels from astronomical objects. Applying adjustments based on calibration frames is called reducing our data.

2.2 Photometry

Photometry is the process of trying to minimize all disparities in stars' images that are not corrected by reducing our data. It takes into account airmass, or the thickness of the atmosphere that each telescope frame was taken through, depending on how low in the sky the target was at the time of observation. We do not observe targets at 30° above the horizon or lower, because observing through more than two airmasses introduces too much noise into our photometry.

2.2.1 Aperture Photometry

To avoid counting photons that come from another source, and just happen to line up with a star in a frame, we use aperture photometry. Two concentric circles are drawn around each star; the photon counts between the two circles are used to

determine an average sky count of non-star photons. Sky counts are subtracted at the calculated rate from the stars' counts.

2.2.2 Differential Photometry

The magnitudes we get from aperture photometry are not true apparent magnitudes. They vary depending on individual frames. Therefore, the magnitudes determined by photometry are differential magnitudes, measured with respect to some baseline that is chosen with respect to stable stars within the frame. If true magnitudes are desired, the true magnitude of some star within the frame must be determined, and true magnitudes of other stars can then be determined through simple arithmetic.

2.3 Telescope and Camera Information

All of our data on these two targets was collected using the 0.4 m David Derick Telescope (DDT) of the Orson Pratt Observatory on Brigham Young University campus. The DDT is equipped with a Newtonian and a Cassegrain focus, but only the Newtonian focus, with a focal ratio of $f/4$, was used to collect data on our targets. The CCD in the DDT is an ST-10 with a plate scale of $0.7''/\text{pixel}$. All analyzed data was taken through a Johnson V filter. Some data for LPH 123 was collected through Johnson B and R filters, but this data has not yet been reduced and analyzed.

Chapter 3

Data Analysis

3.1 Data Acquisition

Data for LPH 123 were collected on 10 nights in the spring and summer of 2007 and 11 nights in the spring and summer of 2008. Data for LPH 127 were collected on two nights in June 2007 and on 13 nights in the spring and summer of 2008. Information about these nights, including their dates and the number of frames taken, is available on Table 3.1. Table 3.2 shows how much of the data from Table 3.1 has been reduced and analyzed.

Table 3.1. Summary of Data Collected

Year	Night	LPH 123 B Filter (frames)	LPH 123 V Filter (frames)	LPH 123 R Filter (frames)	LPH 127 V Filter (frames)	Notes
2007	9-May	58	58	0	0	
	10-May	65	65	0	0	
	16-May	0	55	55	0	
	20-May	0	50	50	0	Not used: filter wheel was switching mid-frame
	26-May	0	100	100	0	Not used: frames were corrupted by bad darks and/or interfering light sources
	1-Jun	0	88	88	0	
	2-Jun	0	80	80	0	
	14-Jun	0	0	0	130	130 frames were also taken in the R filter for LPH 127 - this night only
	19-Jun	0	185	0	0	
	21-Jun	0	0	0	52	
	23-Jun	0	120	0	0	
	11-Jul	0	196	0	0	
	2008	3-Jun	0	15	0	35
10-Jun		0	0	0	170	Not used: data was transferred to a computer beyond my access at the time
13-Jun		24	24	24	0	Not used: data was transferred to a computer beyond my access at the time
17-Jun		0	68	0	0	Not used: data was transferred to a computer beyond my access at the time
19-Jun		26	26	26	160	
20-Jun		0	120	0	55	
25-Jun		20	20	20	0	
26-Jun		0	0	0	70	
27-Jun		0	0	0	180	
3-Jul		10	10	10	125	Not used: ap_obhead script gave an error
4-Jul		20	20	20	70	
8-Jul		0	0	0	90	
10-Jul	24	24	24	50		
11-Jul	20	20	20	60		

Table 3.1

Year	Night	LPH 123 B Filter (frames)	LPH 123 V Filter (frames)	LPH 123 R Filter (frames)	LPH 127 V Filter (frames)	Notes
	24-Jul	0	0	0	60	
	31-Jul	0	0	0	95	
	1-Aug	0	140	0	150	

Table 3.2. Summary of Data Reduced and Analyzed

Year	Night	LPH 123 V Filter (frames)	LPH 127 V Filter (frames)	Notes
2007	9-May	56	0	Two frames excluded: oversaturation
	10-May	65	0	
	16-May	55	0	
	1-Jun	88	0	
	2-Jun	80	0	One frame excluded: made apphot crash
	14-Jun	0	129	
	19-Jun	185	0	
	21-Jun	0	52	
	23-Jun	120	0	
	11-Jul	196	0	
2008	19-Jun	26	160	
	20-Jun	120	55	
	25-Jun	20	0	
	26-Jun	0	70	
	27-Jun	0	180	
	4-Jul	20	70	
	8-Jul	0	90	
	10-Jul	24	50	
	11-Jul	20	60	
	24-Jul	0	60	
1-Aug	140	150		

3.2 Reduction by Script

Our data was processed, including reducing the data by applying calibration frames, was done using the Image Reduction and Analysis Facility program (IRAF). In addition, we used a set of scripts known as the Swenson-Iverson Data Analysis Package (SIDAP) (Swenson (2008), Iverson (2008)). SIDAP was written by Craig Swenson and E. Paul Iverson in 2008, and at the time of writing can be found at [this linked Internet address](#). It is intended to make IRAF analysis more precise, as well as streamline some steps of the process to make things easier for the user. Many of the SIDAP scripts are built on the assumption that you have run all the previous SIDAP

scripts in preparation for them, so they are best used as a complete package. SIDAP contains the following scripts:

- **ap_rfits:** This script applies the IRAF command “rfits” to each file, and makes sure all files are named with a uniform convention that lets subsequent scripts recognize them.
- **ap_obhead:** This script puts necessary information into the “header” file that goes with each frame, so that subsequent frames can use the information contained in these headers. This script automates the use of the traditional IRAF commands “asthedit,” “setairmass,” and “setjd.” It also supplies or asks the user to supply any information that IRAF would otherwise locate in a .cmds file.
- **ap_calhead:** This script updates calibration frames’ headers with the correct information in the IMAGETYP, OBJECT, and SUBSET fields.
- **ap_pierside:** This script classifies object frames as being in the east or west half of the sky, so that frames on one side of the sky may later be rotated to match their counterparts. If the script cannot tell which side of the sky the image came from by its hour angle, it prompts the user to inform it.
- **ap_gain_rdnoise:** This script calculates the gain and rdnoise rates of the CCD and adds these statistics to frames’ headers. This information is used by subsequent scripts to improve the processes of applying calibration frames and performing photometry. The gain statistic represents a phenomenon where a CCD pixel will sometimes count more than one event when it is hit by one photon. The rdnoise statistic represents when a photon strikes one pixel but is counted by another pixel as the pixels’ signals are processed towards the CCD’s readout points.
- **ap_proc:** This script automates the use of the traditional IRAF commands “zerocombine,” “darkcombine,” and “flatcombine,” making necessary adjustments

to the commands' parameters in between uses, in order to apply all calibration frames.

- **ap_skynoise:** This script calculates the average skynoise for the frame, based on the skynoise in a radius around 50 objects throughout the frame. The skynoise is recorded in the frame's header file and is used later by the align and apphot scripts.
- **ap_fwhm:** This script calculates the full width half max statistic of the brighter stars in each frame in order to determine the ideal aperture size to use in the photometry process. Apphot defaults to an aperture radius based on this statistic if it is unable to calculate a good aperture radius using psfmeasure.
- **ap_trim:** This script removes the 10 outer pixels from each frame to avoid overscan regions that would hinder DAOfind.
- **ap_rotate:** This script rotates frames taken on one side of the telescope's pier by 180 degrees (or by another amount, as the user dictates), so that they will match the orientation of frames taken on the other side of the pier. This script is optional if all frames being analyzed were taken with the same orientation.
- **ap_align:** This script uses DAOfind to analyze the layout of each frame and aligns a number of frames so that stars are located in the same places on all of them. Without running this script, all object frames within the same night tend to be centered on slightly different points in the sky, due to the telescope's inability to perfectly track the movement of the celestial sphere. This script also creates clear artificial borders, if necessary, on the edges of adjusted frames, so that their new borders will line up with the borders of other frames. Aligning all frames makes it much easier to automate the photometry process in the final script.

- **ap_apphot:** This script automates the use of the traditional “apphot” IRAF command to perform photometry on reduced object frames.

3.3 Statistical Analysis

We used a program called VARSTAR 5, written by Dr. Eric Hintz ([Hintz et al. \(1997\)](#)), to turn the output of the ap_apphot script into a series of differential magnitudes. VARSTAR helps figure out which stars, out of the possible comparison stars that were processed by apphot, are constant enough to be good comparison stars, against which the differential magnitude of our target star can be measured. VARSTAR takes the relative magnitudes that were calculated by apphot for each frame of each night, for each star, and finds the standard deviation of their distribution in units of magnitude. It then reports this standard deviation to the user, calling it the error for the star, and allows the user to remove stars with high errors from the calculation of differential magnitudes. After running several iterations of VARSTAR, the differential magnitudes of the stars can be calculated based on stars that have an error of 0.02 or less, hopefully as low as 0.008, which are probably stable stars that make for good comparisons. At each iteration, VARSTAR also adjusts the stars’ reported differential magnitudes so that the stars used in the calculation have an average magnitude of zero.

VARSTAR creates output in the form of data files from each star that contain the star’s differential magnitude at each time (measured in units of Heliocentric Julian Days, or HJD) that a frame was taken. These output files can be used to graph differential magnitudes as a function of time.

Table [3.3](#) shows the stars that VARSTAR kept in its determination of differential magnitudes for each night of data.

3.4 Initial Analysis

Fig. [3.1](#) shows a typical night of VARSTAR results.

Table 3.3. Comparison Stars Retained by
VARSTAR

Year	Night	Target	Stars Kept
2007	9-May	LPH 123	2, 5, 14, 17, 19
	10-May	LPH 123	2, 5, 17, 19
	16-May	LPH 123	2, 5, 14, 20
	1-Jun	LPH 123	4, 9, 12, 16, 19
	2-Jun	LPH 123	4, 9, 17, 19
	14-Jun	LPH 127	2, 3, 5, 7
	19-Jun	LPH 123	2, 4, 14, 17, 19
	21-Jun	LPH 127	2, 3, 4, 5, 7, 9, 10
	23-Jun	LPH 123	2, 5, 9, 12, 17
	11-Jul	LPH 123	2, 5, 14, 17
	2008	19-Jun	LPH 123
19-Jun		LPH 127	2, 3, 4, 5
20-Jun		LPH 123	2, 5, 9, 14
20-Jun		LPH 127	2, 3, 4, 5
25-Jun		LPH 123	4, 6, 9, 14, 17
26-Jun		LPH 127	2, 3, 4, 5
27-Jun		LPH 127	2, 3, 4, 5, 7
4-Jul		LPH 123	2, 4, 5, 9, 14, 17, 19, 20
4-Jul		LPH 127	3, 5, 10, 11
8-Jul		LPH 127	2, 3, 4, 5
10-Jul		LPH 123	4, 9, 14, 17
10-Jul		LPH 127	2, 3, 4, 5
11-Jul		LPH 123	4, 9, 14, 17
11-Jul		LPH 127	2, 3, 4, 5
24-Jul		LPH 127	2, 3, 4, 5
1-Aug		LPH 123	2, 14, 17, 19
1-Aug		LPH 127	2, 4, 6, 9

Each star that was determined by VARSTAR to be a comparison star for this night has a very nice, flat line, showing it to have a very stable magnitude throughout the night. LPH 123 also appears to have been very stable. A graph of differential magnitudes for LPH 123 alone reveals that it did indeed vary during this night, but only in very small magnitude differences and without any consistent pattern (Fig. 3.2):

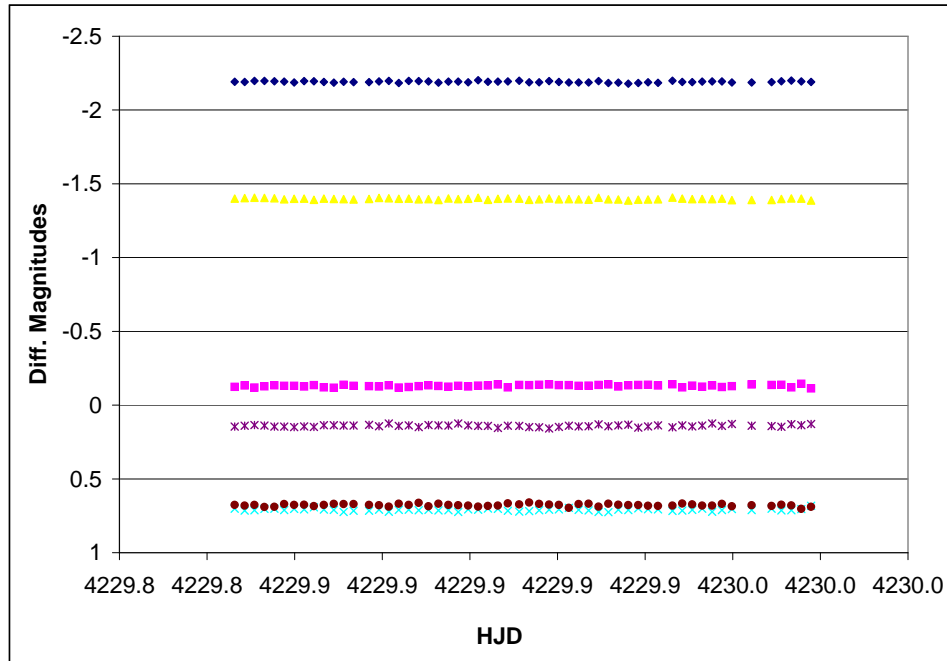


Figure 3.1: LPH 123 and Comparison Stars, May 9, 2007: A typical night, showcasing the flat lines of stars that are stable, at least on a short-term scale. Blue diamonds are LPH 123, pink squares are Star 2, yellow triangles are Star 5, cyan x's are Star 14, violet asterisks are Star 17, and red circles are Star 19.

This lack of a noteworthy pattern in LPH 123's magnitude is not surprising, since we are expecting to find that it is a long-period variable, and do not expect to see much variation in its magnitude within the course of one night.

Graphs from two other nights are presented (Fig. 3.4, Fig. 3.4) to support this conclusion, since we want to cover the possibility that LPH 123 could be a β Cephei pulsator.

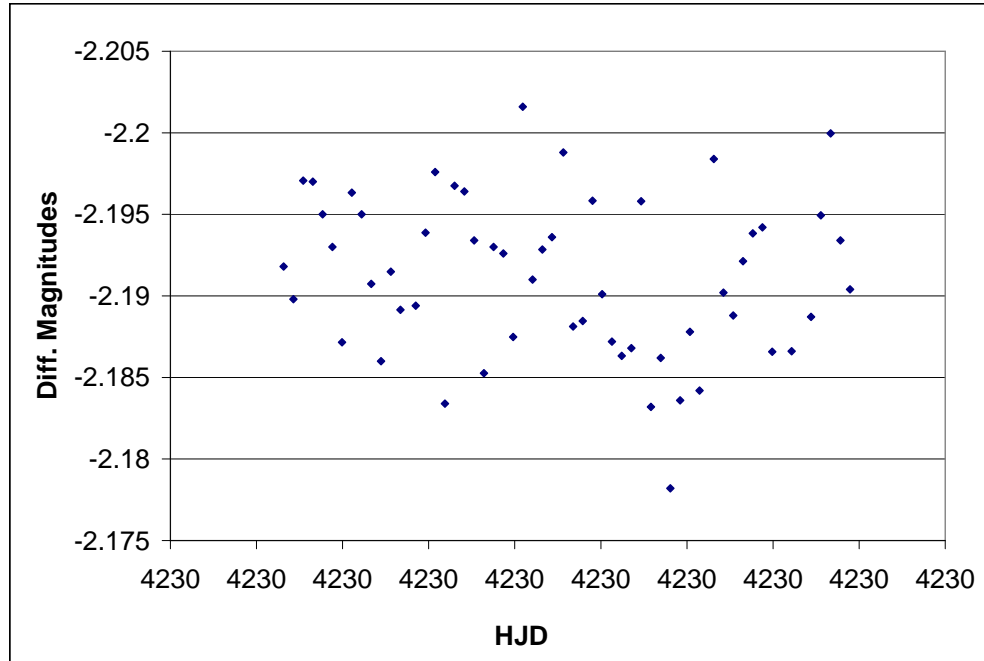
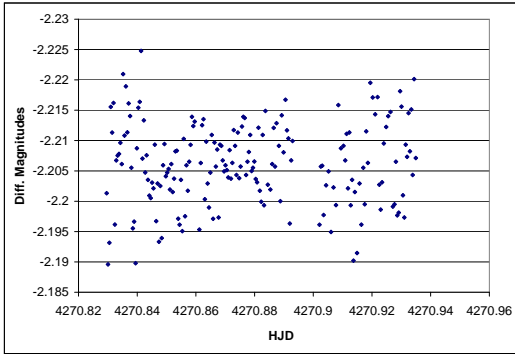


Figure 3.2: LPH 123, May 9, 2007: No light curve reminiscent of a variable star is visible in the span of a few hours.

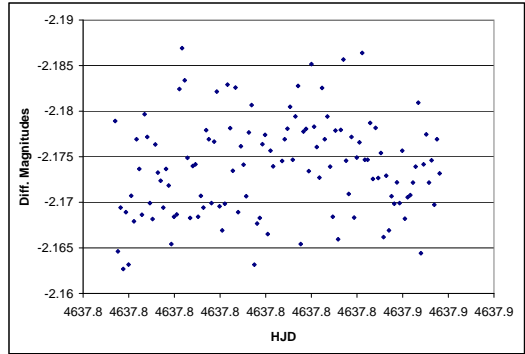
Similar graphs for LPH 127 are presented (Fig. 3.4, Fig. 3.4, Fig. 3.4):

3.5 Unusually Noisy Data

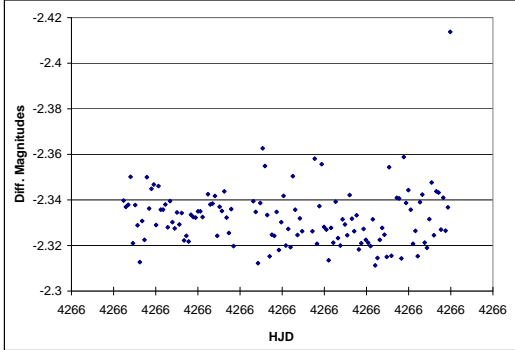
Sometimes the formulas used in the photometry process are unable to return a meaningful result of a star's magnitude, especially if a star appears unusually faint or not round-shaped on a given frame. In this case, IRAF returns a result of "indefinite" for a star's magnitude in a given frame. The `ap_apphot` script replaces this indefinite result with a sufficiently high number, so that VARSTAR can accept this input. Indefinite results were clearly identifiable in our data as data points with a differential magnitude of at least 60 reported.



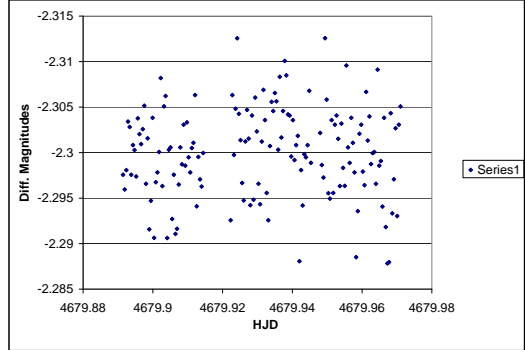
LPH 123, June 19, 2007



LPH 123, June 20, 2008



LPH 127, June 14, 2007



LPH 127, August 1, 2008

Figure 3.3: Four more graphs of typical one-night light curves are presented. Though the one on the top left has an interesting shape, suggesting that noise conditions were less during the middle of that night of data, none of these look like a repeating variable pattern.

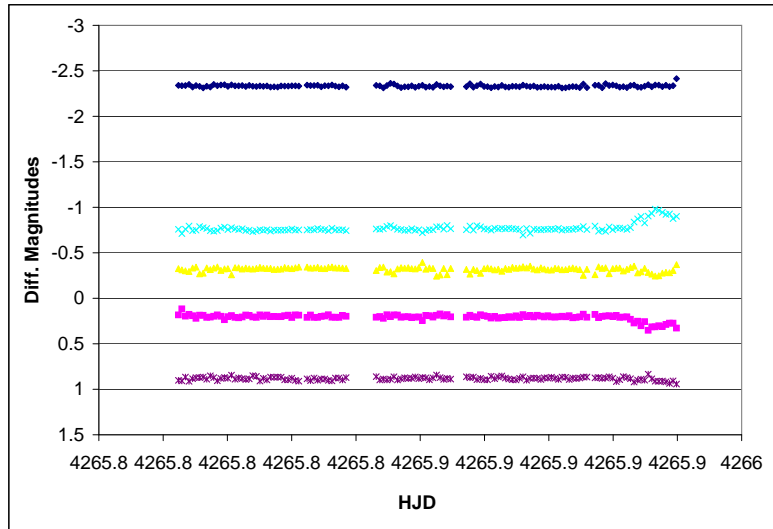


Figure 3.4: LPH 127 and Comparison Stars, June 14, 2007: A typical night, showcasing the flat lines of stars that are stable, at least on a short-term scale. Blue diamonds are LPH 127, pink squares are Star 2, yellow triangles are Star 3, cyan x's are Star 5, and violet asterisks are Star 7.

The presence of indefinite results is nothing unusual. However, in our data, they appeared more often than expected.

In addition, certain stars on certain nights contained a strange number of clear outlier data points, even if they had very few indefinite results, as demonstrated in Fig. 3.5. There were two indefinite points for Star 3 on this night, which had given values between 88 and 89; they have been eliminated from this data set. The anomalous data points on this graph are much harder to explain.

If these noisy data points weren't present on comparison stars, we could ignore them and focus only on analyzing data for LPH 123 and 127 and their comparison stars. However, the difficulty arises from certain stars that are excellent comparison stars some nights, and yet are filled with noisy data points on other nights. In fact, every star in the field of LPH 123 has at least one night of unusually noisy data, when it can't be used as a comparison star. This means, when we try to set the differential magnitudes from different nights on the same scale with respect to some

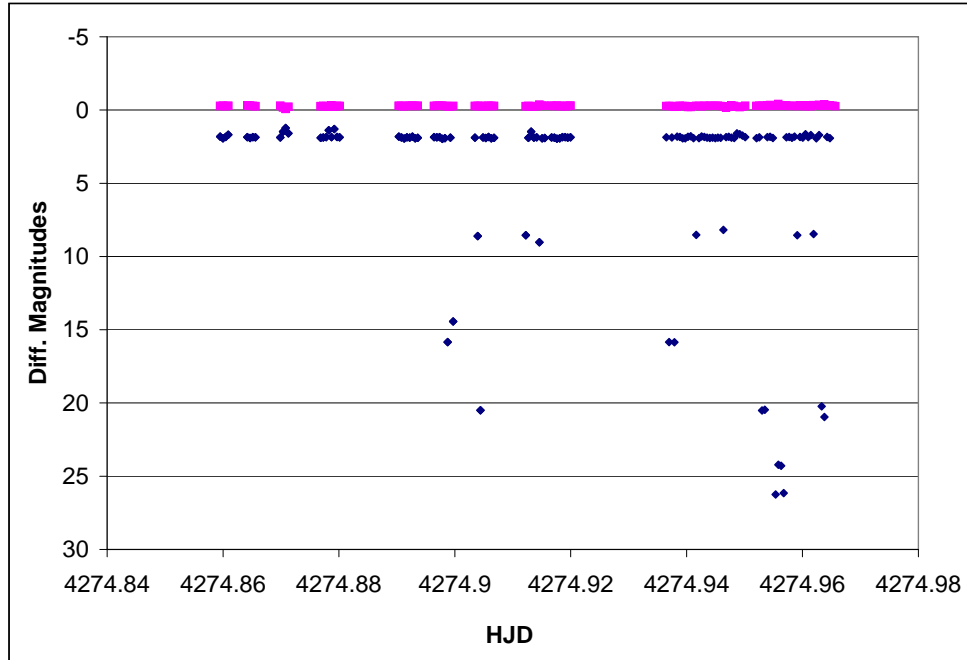


Figure 3.5: Demonstration of Outliers, Field of LPH 123, June 23, 2007: Blue diamonds are Star 3 and pink squares are Star 17. The data points on this graph above differential magnitude 5 are clearly anomalous, even though they are not caused by indefinite results.

stable zeropoint, that it's difficult to know if any comparison stars can be trusted as completely stable representations of that zeropoint.

These outliers also cause a problem in seeing overall trends of stars when multiple nights are graphed on the same graph. Whole nights of data get crammed into a couple pixels on the x-axis of a multiple-night graph. This is not an unusual difficulty in tracking stars over multiple nights; however, the difficulty is compounded by the presence of extra outlier data points. For example, when we graph several nights of data from LPH 123, summer 2008, without removing outlier data points (other than indefinite results), we get a graph like Fig. 3.6.

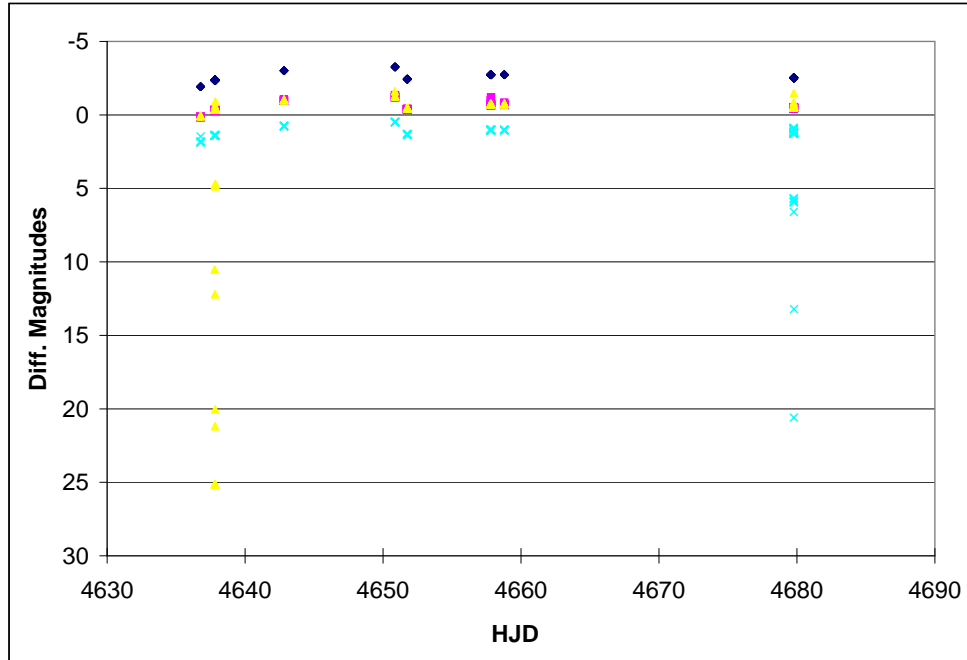


Figure 3.6: Demonstration of Vertical “Lines”, Field of LPH 123, June 19-August 1, 2008

3.6 Multiple-Night Analysis

We attempted to make the stable stars all line up from night to night by adjusting each night with respect to a zeropoint. For convenience, we chose the median point of the first night of data as our zeropoint for each target.

We made a table of the median data point of each comparison star on each night. Then, for each star, we took the difference between its median on the first night and its median on the night to be adjusted. We threw out any comparison stars each night that had particularly anomalous data, then took the mean or the median of the calculated differences, using all remaining comparison stars. The resulting average was the value we used to adjust the entire night’s data to the zeropoint in order to compare it with other nights.

Fig. 3.7 shows the resulting data for LPH 123’s comparison stars over the entire course of our study. For each star and each night, a median data point is shown,

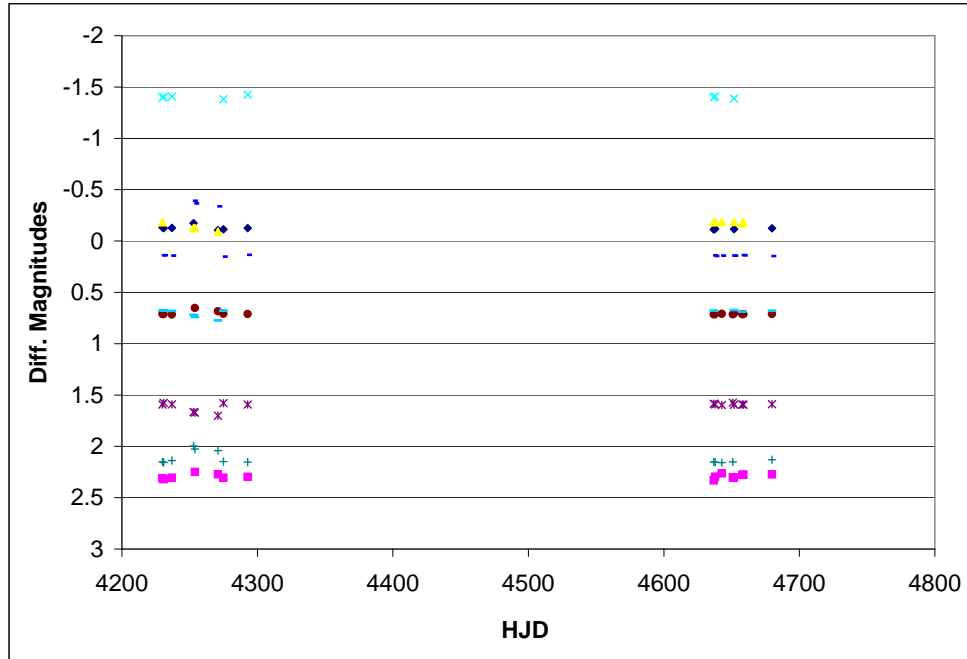


Figure 3.7: Visualization of Zero-point Adjustments, Comparison Stars of LPH 123 (Median Points of Each Night): Blue diamonds are Star 2, pink squares are Star 3, yellow triangles are Star 4, cyan x's are Star 5, violet asterisks are Star 9, red circles are Star 14, green crosses are Star 16, short blue hyphens are Star 17, and longer cyan hyphens are Star 19. This graph shows the effectiveness of our calculated zero-point adjustments.

so outlier data points won't obscure the overall effect of the zero-point adjustment.

Fig. 3.8 shows the same result for LPH 127's comparison stars.

Adjusted to the zero-point, these lines of comparison star data still aren't ideal lines, especially in the field of LPH 123. The change in differential magnitudes between supposedly stable comparison stars is greater than expected from night to night. In particular, data from June 1, June 2, and June 19, 2007, don't line up perfectly with data from other nights. The deviation of Star 5 (in the field of LPH 123) from its usual magnitude on these nights, relative to the other comparison stars,

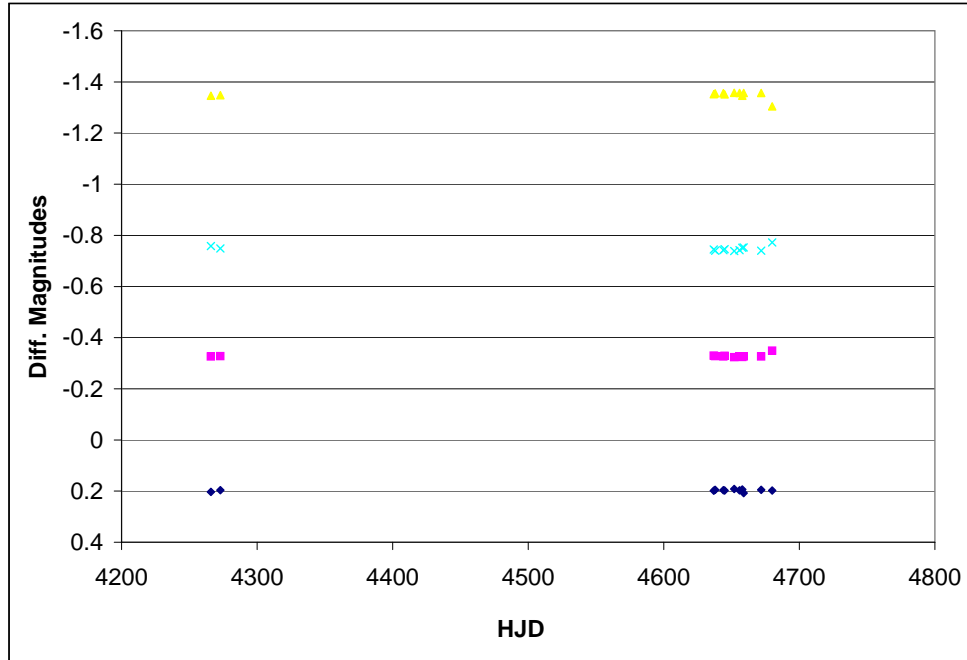


Figure 3.8: Visualization of Zeropoint Adjustments, Comparison Stars of LPH 127 (Median Points of Each Night): Blue diamonds are Star 2, pink squares are Star 3, yellow triangles are Star 4, and cyan x's are Star 5. This graph shows the effectiveness of our calculated zeropoint adjustments.

is great enough that it bears further investigation whether this star is itself a long-period variable. Overall, though, the comparison stars form, on average, straight lines from night to night with the calculated zeropoint values.

3.7 Phased Analysis

With zeropoint adjustments, we can see some variations from night to night in our actual target stars. See Fig. 3.9 and Fig. 3.10. Also see Fig. 3.11 and Fig. 3.12, where only median points for each night are shown in order to mitigate the distracting effect of outlier data points.

With this data, we are able to see at least one promising variation in our HMXB data. LPH 123 appears to have a peak in brightness in early June 2007. However, the small variations we see might also be caused by imperfect zeropoint

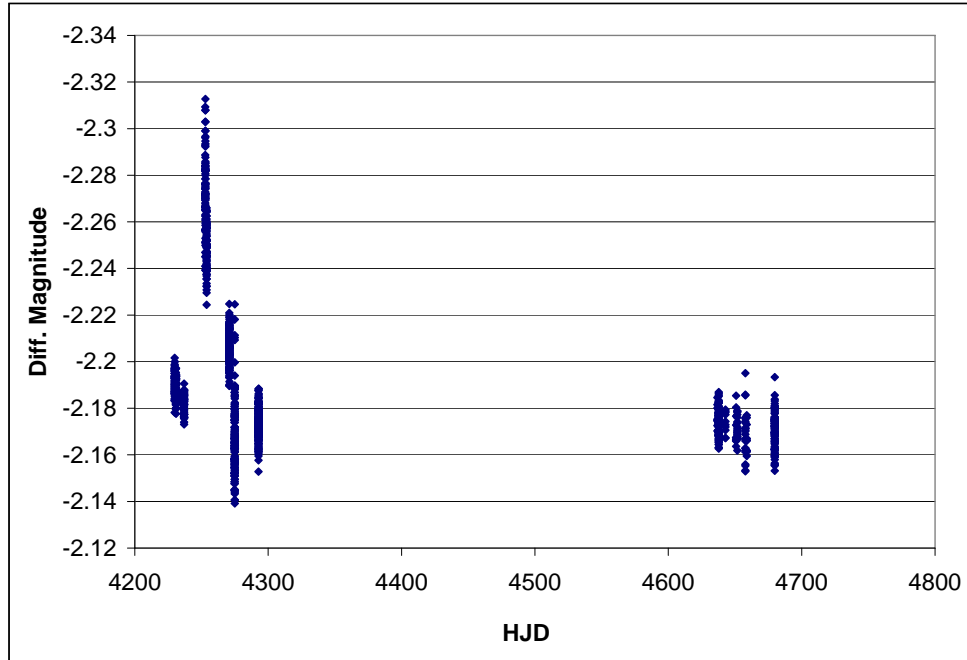


Figure 3.9: LPH 123 over 16 Nights

adjustments. It is not clear from these graphs whether these HMXBs exhibit any cyclical behavior. Variations we see aren't repeating. That might just be due to the period of variation being longer than the duration of this study, but it might mean there is some repetitive behavior that is just too low-amplitude to see on these graphs.

To see if there are actually cyclical trends in these stars' light curves, we put this data into a program called Period04, which analyzes the data points with Fourier analysis and tells us if our data can be approximated by any periodic functions. Then we make phased graphs, where all of our data is partitioned into widths equal to the period given by Period04. We then made graphs based on the data points' phase within these partitions.

Details of Period04 results can be found in [Appendix A](#).

Phased LPH 123 Results: [Figure 3.13](#)

Phased LPH 127 Results: [Figure 3.14](#)

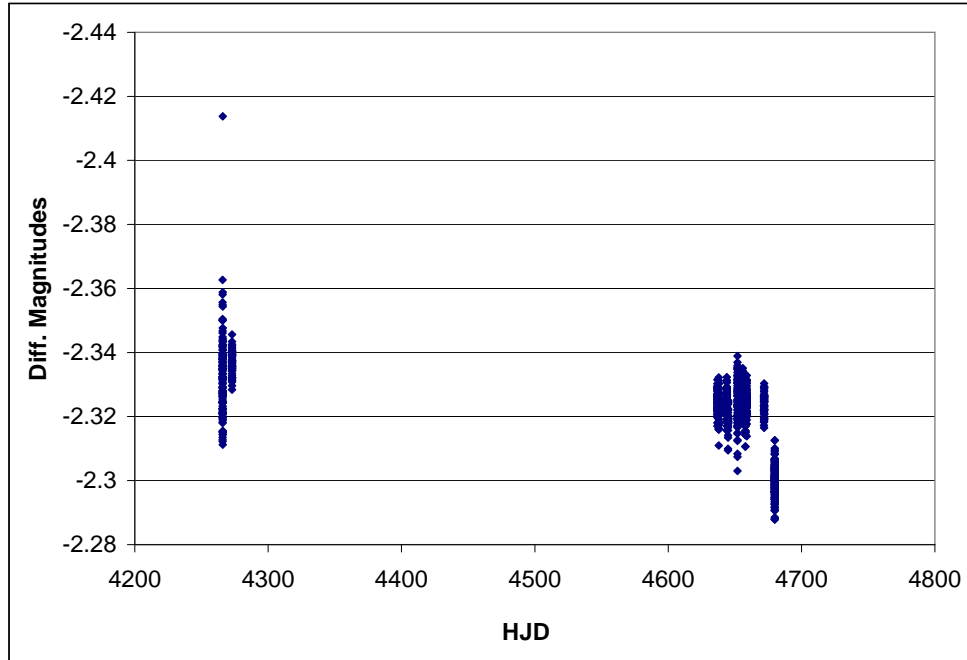


Figure 3.10: LPH 127 over 12 Nights

While there are certainly some small variations in these graphs, which may indicate variability, the variations are too small and do not form clear enough patterns to fill us with any confidence in these periods. The large empty spaces on these phased plots would have to be filled in with data that supports the overall possible trends we see for us to conclude that these represented actual oscillations. In addition, the fact that the periods represented here are on a scale of days, rather than weeks or months like we expect for a long-period HMXB, makes us suspect that these are accidental periods, rather than anything our targets are actually doing. In effect, Period04 just gave us the best guess it could, given data that did not actually have periodic behavior.

Attempting to find a periodic pattern in the magnitudes of Star 5 was similarly inconclusive: [Figure 3.15](#)

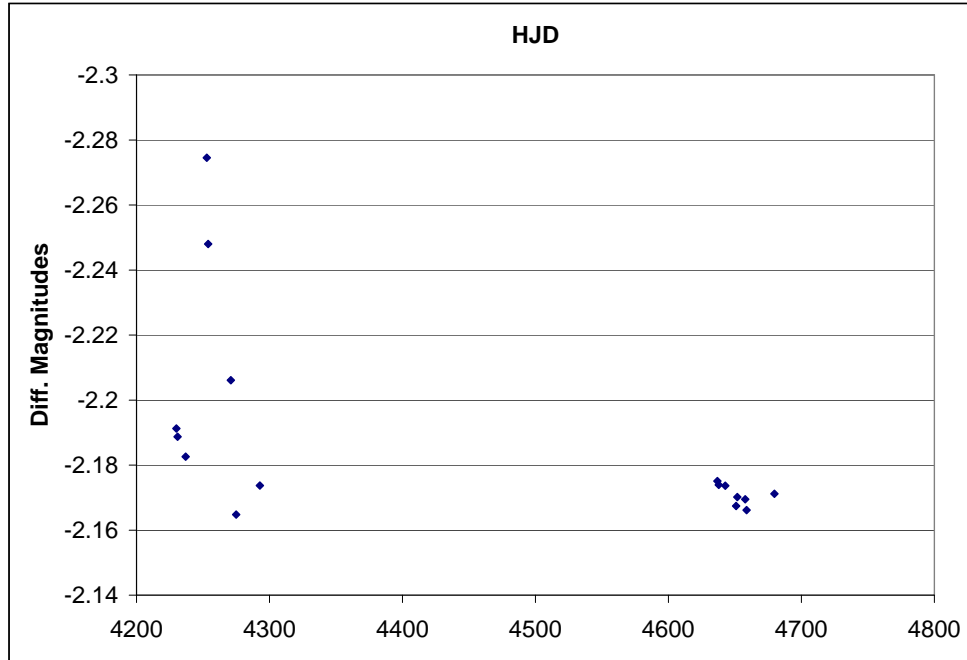


Figure 3.11: LPH 123 over 16 Nights (Median Points of Each Night)

3.8 Additional Graphs

To further clarify our results, we have included a few more graphs, showing different perspectives on the results we have already discussed.

Figure 3.8 and Figure 3.8 show light curves for LPH 123, separated by year. This lets us see a little more detail along the x-axis. Two comparison stars are also shown, so that the graphs' y-axes will have a scale that makes changes meaningful.

Figure 3.8 identifies LPH 123's Comparison Star number 5, which we have discussed so much as being a candidate for further research. An additional graph of this star in 2007, when its movement seems to have been most interesting, is also provided without phasing (Fig. 3.8).

Finally, in a similar vein, we present LPH 127 and its comparison stars, using only data from 2008 (Fig. 3.18).

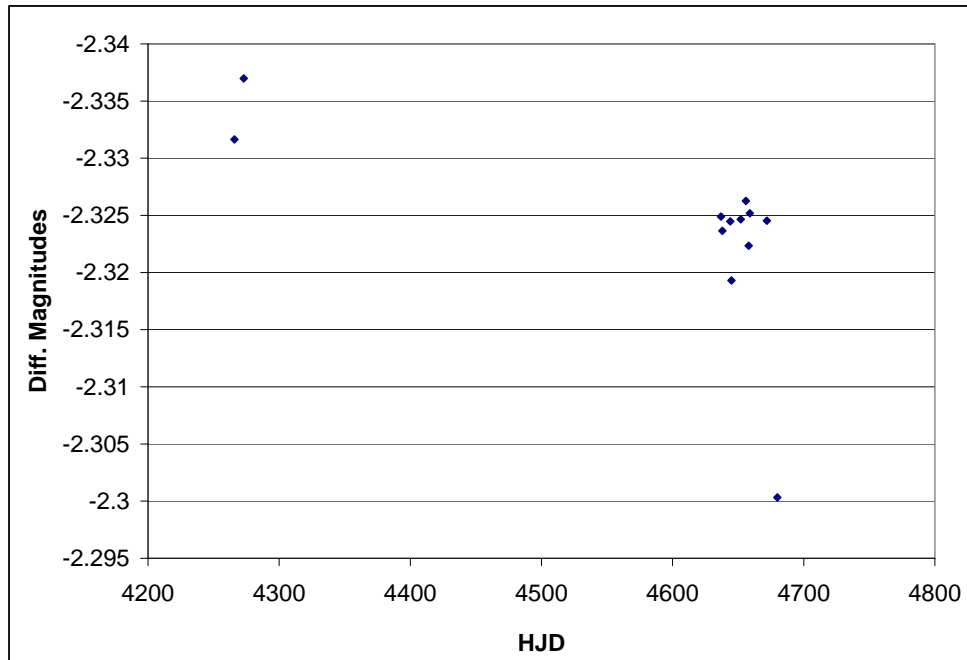


Figure 3.12: LPH 127 over 12 Nights (Median Points of Each Night)

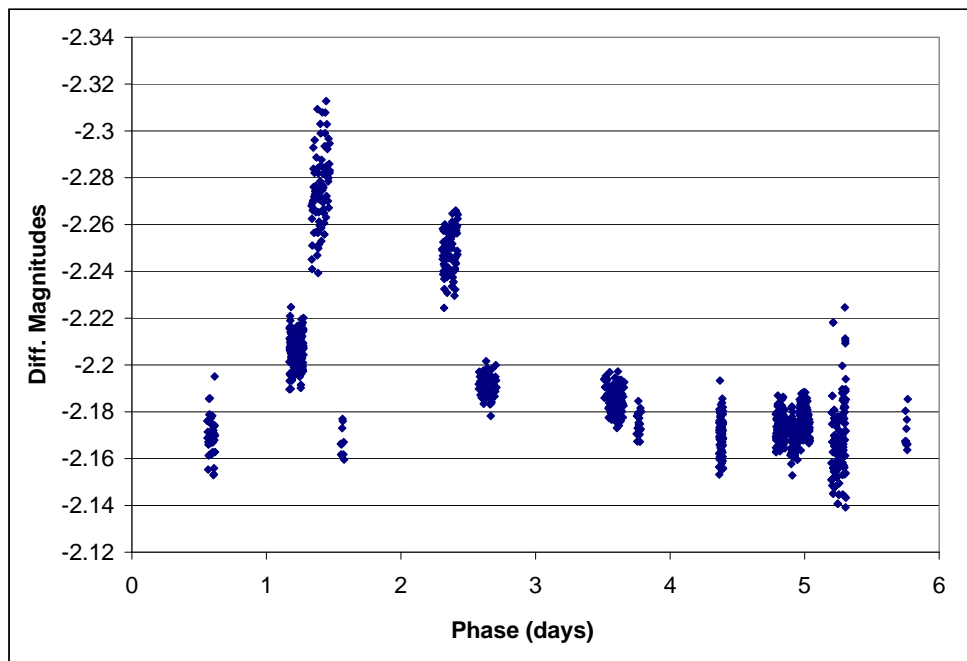


Figure 3.13: LPH 123 Phased Data; Calculated Period: 6.055704 Days. If Period04 was able to detect a repeating periodicity in this star's light curve, it should show up as a pattern on this graph.

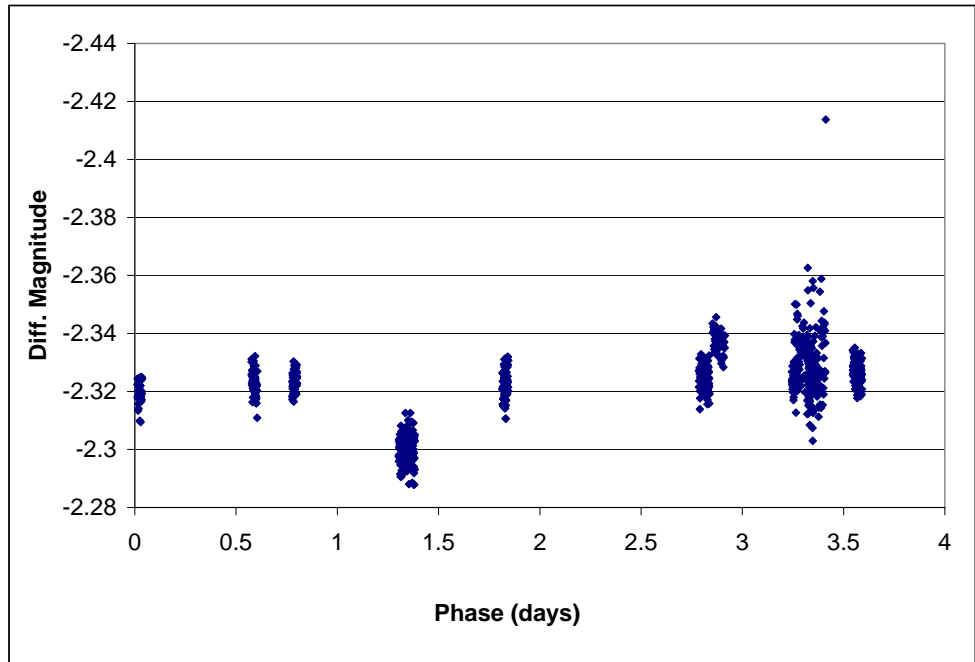


Figure 3.14: LPH 127 Phased Data; Calculated Period: 3.74829 Days. If Period04 was able to detect a repeating periodicity in this star's light curve, it should show up as a pattern on this graph.

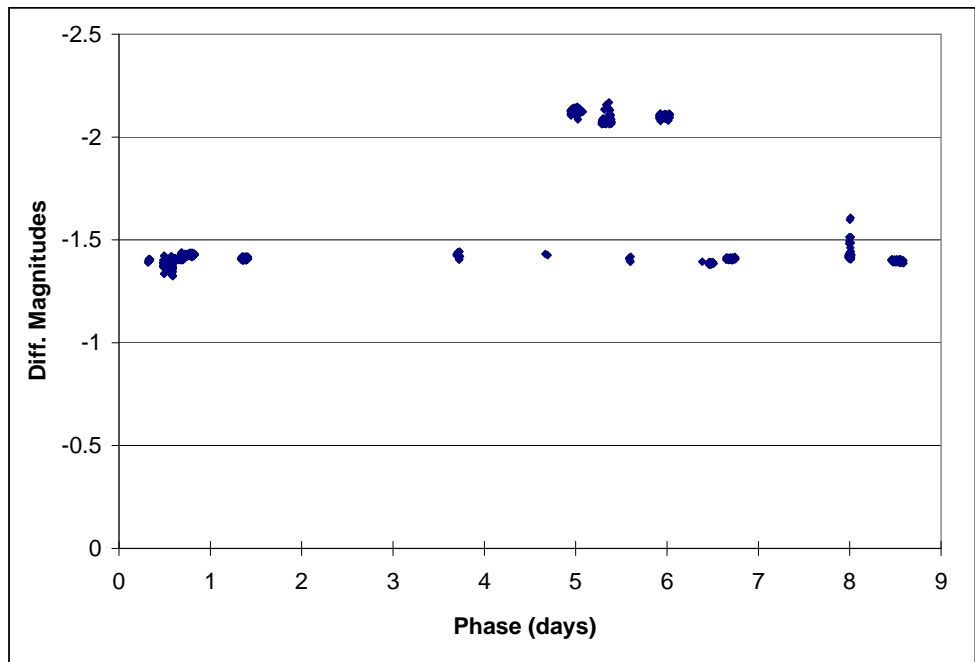
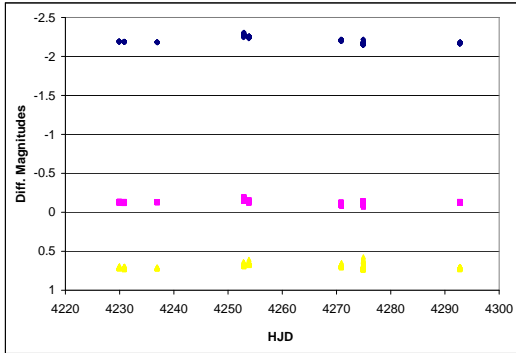
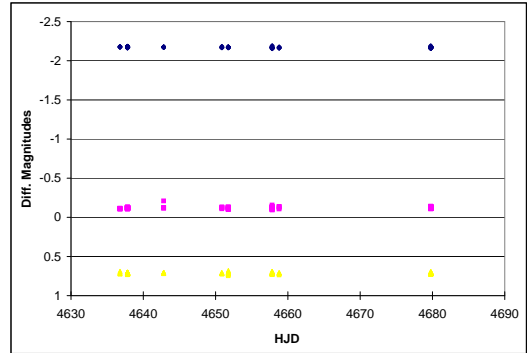


Figure 3.15: Star 5 Phased Data, Field of LPH 123; Calculated Period: 8.83100 Days. If Period04 was able to detect a repeating periodicity in this star's light curve, it should show up as a pattern on this graph.



**LPH 123
and Two Comparison Stars
May 9-July 11, 2007**

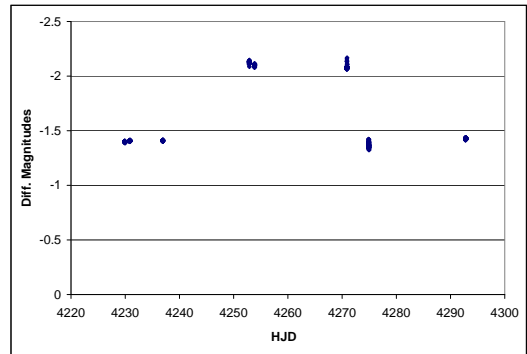


**LPH 123
and Two Comparison Stars
June 19-August 1, 2008**

Figure 3.16: Blue diamonds are LPH 123, pink squares are Star 2, and yellow triangles are Star 14. Note that, while its amplitude is small, LPH 123's increase in luminosity in early June 2007 is still visible on this graph with respect to its comparison stars.



LPH 123 is the bright star
near the center of the frame.
Star 5 is marked by a blue halo.



**Star 5
Field of LPH 123
May 9-July 11, 2007**

Figure 3.17: Information for the benefit of future studies of Comparison Star 5.

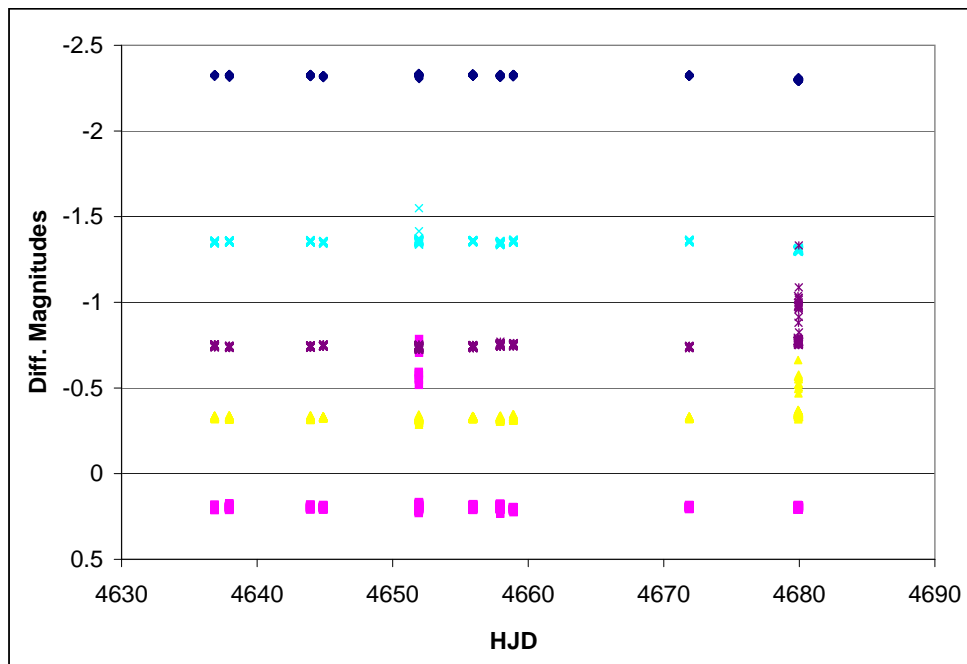


Figure 3.18: LPH 127 and Comparison Stars, June 19-August 1, 2008: Blue diamonds are LPH 127, pink squares are Star 2, yellow triangles are Star 3, cyan x's are Star 4, and violet asterisks are Star 5.

Chapter 4

Conclusions

4.1 Results

Period04's inability to detect any convincing periodicity means we can only suspect that the data we have collected for LPH 123 and 127 represents, essentially, one iteration or less of any significant variations.

We conclude that LPH 123 is probably a long-period variable star, as expected, but we cannot determine a period for its variations. LPH 127 may still be a variable star as well. The nature of long-period HMXBs is such that they may only manifest significant variations during periastron, which may have occurred for our targets during the time span between July 2007 and June 2008, or may occur too seldom for us to have seen during this study at all.

4.2 Further Research

The telescope data used in this study should be examined frame-by-frame. It is possible that some bad frames escaped detection and led to the unusual quantity of noisy data in our analysis.

Data on LPH 123 and 127 need to continue being collected and added to the data that we collected. With more data, it will be more clear whether frequencies from Period04 actually lead to any kind of pattern on phased plots. We may also get some good pictures of these systems near periastron and see more clear movements than our current data shows.

Further research should also monitor Star 5 in the field of LPH 123. If it shows variation in magnitude aside from that seen on June 1, 2, and 19, 2007, it should be dropped as a comparison star.

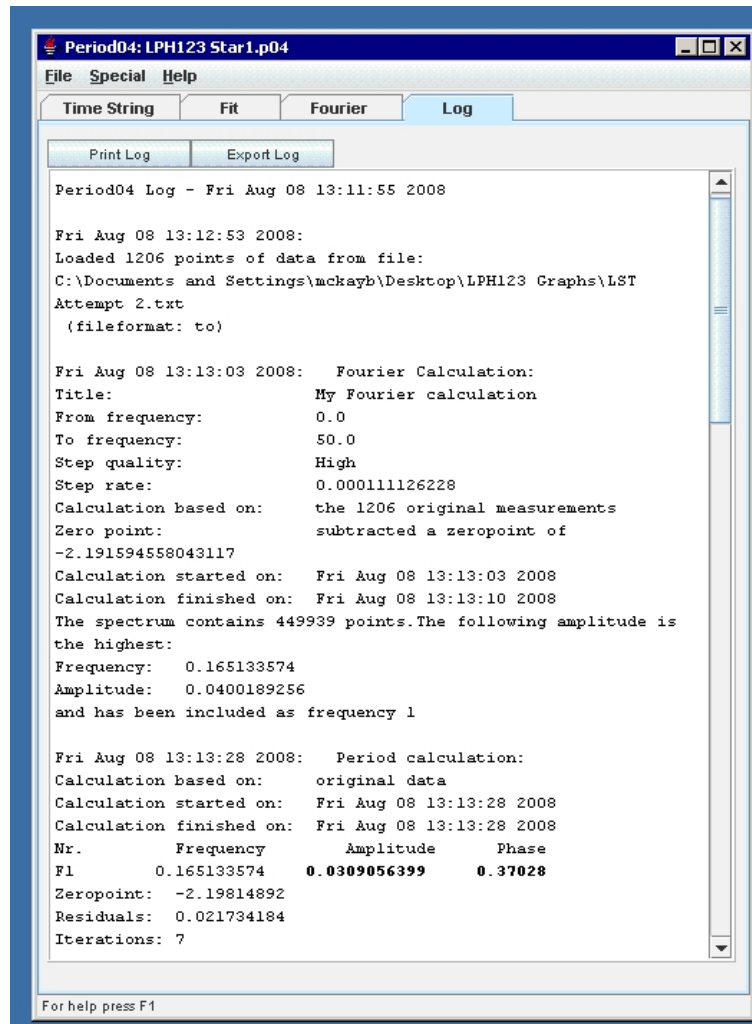
References

- Hintz, E. G. and Jonev, M. D. and McNamara, D. H. and Nelson, K. A. and Moody, J. W. and Kim, C., PASP, 1997, 109, 15-20
- Iverson, E. P., Department of Physics and Astronomy Brigham Young University Senior Thesis, 2008
- Liu, Q. Z. and van Paradijs, J. and van den Heuvel, E. P. J., A&AS, 2000, 25-49
- Sarty, G. E. and Kiss, L. L. and Huziak, R. and Wu, K., Journal of the American Association of Variable Star Observers (JAAVSO), 2006, 56
- Swenson, C., Department of Physics and Astronomy Brigham Young University Senior Thesis, 2008

Appendix A

Period04 Log Excerpts

Screenshots of the most important information from Period04 are pictured in Figure A.1 and Figure A.2.



```
Period04: LPH123 Star1.p04
File Special Help
Time String Fit Fourier Log
Print Log Export Log
Period04 Log - Fri Aug 08 13:11:55 2008

Fri Aug 08 13:12:53 2008:
Loaded 1206 points of data from file:
C:\Documents and Settings\mckayb\Desktop\LPH123 Graphs\LST
Attempt 2.txt
(fileformat: to)

Fri Aug 08 13:13:03 2008: Fourier Calculation:
Title: My Fourier calculation
From frequency: 0.0
To frequency: 50.0
Step quality: High
Step rate: 0.000111126228
Calculation based on: the 1206 original measurements
Zero point: subtracted a zeropoint of
-2.191594558043117
Calculation started on: Fri Aug 08 13:13:03 2008
Calculation finished on: Fri Aug 08 13:13:10 2008
The spectrum contains 449939 points. The following amplitude is
the highest:
Frequency: 0.165133574
Amplitude: 0.0400189256
and has been included as frequency 1

Fri Aug 08 13:13:28 2008: Period calculation:
Calculation based on: original data
Calculation started on: Fri Aug 08 13:13:28 2008
Calculation finished on: Fri Aug 08 13:13:28 2008
Nr. Frequency Amplitude Phase
F1 0.165133574 0.0309056399 0.37028
Zeropoint: -2.19814892
Residuals: 0.021734184
Iterations: 7

For help press F1
```

Figure A.1: Period04 Log for LPH 123

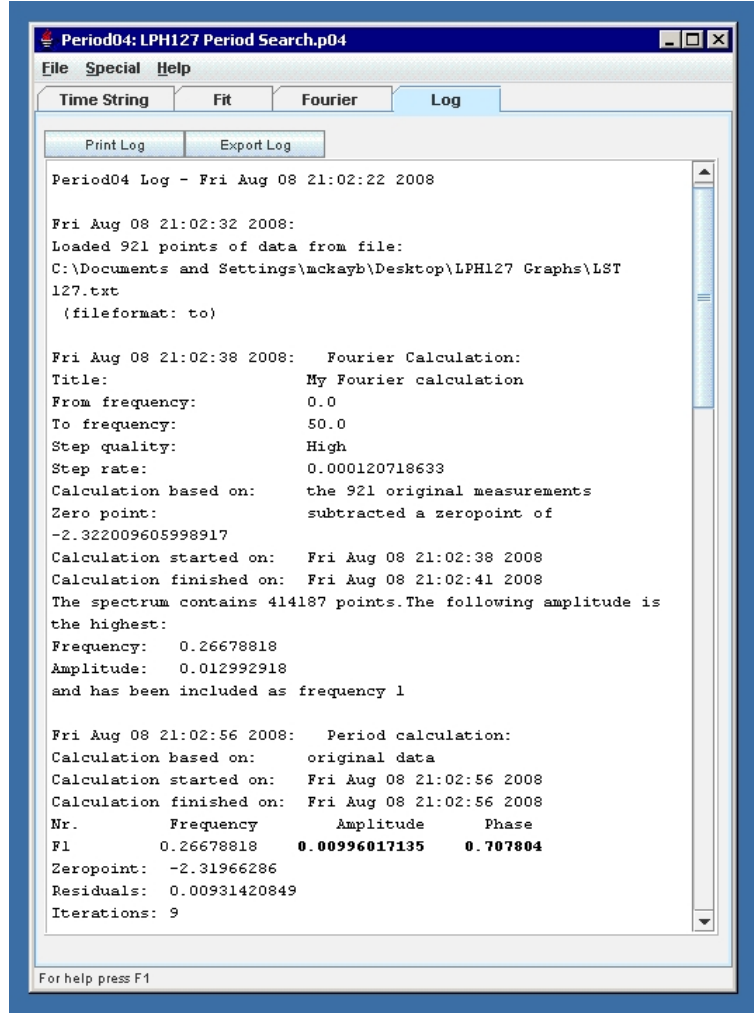


Figure A.2: Period04 Log for LPH 127